Electrochemical corrosion behavior of LDX 2101® duplex stainless steel in a fluoridecontaining environment

Electrochemical corrosion behavior of LDX 2101® duplex stainless steel in a fluoride-containing environment

F. Rosalbino*, G. Scavino, G. Ubertalli

Politecnico di Torino, Dipartimento di Scienza Applicata e Tecnologia (DISAT), Corso Duca degli Abruzzi 24, I-10129 Torino (Italy),

Abstract

The effect of fluoride on the electrochemical corrosion behaviour of a LDX 2101® duplex stainless steel (DSS) was studied. Open circuit potential, E_{OC}, and electrochemical impedance spectroscopy (EIS) measurements were carried out in artificial saliva and with the addition of fluoride (1 *wt.*% NaF). The electrochemical corrosion behaviour of the AISI 316L austenitic stainless steel (SS) was also evaluated for comparison. Both open circuit potential and EIS results indicate that DSS and austenitic SS undergo spontaneous passivation due to spontaneously formed oxide film passivating the metallic surface, in the simulated aggressive environments. However, LDX 2101® exhibits superior corrosion resistance as compared to AISI 316L, and this improvement is ascribed to the formation of a passive film which shows higher protective effectiveness than the one formed on AISI 316L.

Key words: Duplex stainless steel; Fluoride; Corrosion behaviour; Electrochemical impedance spectroscopy (EIS); Passive film

* Corresponding author. tel: 0039110904760, fax: 0039110904699

E-mail address: francesco.rosalbino@polito.it (F. Rosalbino)

1. Introduction

The total cost and environmental consequences of corrosion problems have become a major challenge to engineers to reduce economic losses [1]. Austenitic stainless steels (SS) are used for a wide range of technological applications including orthodontic treatments. Metallic orthodontic appliances consist of bands, arch wires, ligature wires, hooks, tubes, brackets and springs. Type AISI 316L stainless steel is the most commonly used orthodontic appliances material with a typical composition in mass fractions of 17% chromium, 10% nickel, 2-3% molybdenum, balanced with iron and minor elements, such as manganese, carbon, silicon [2]. Austenitic stainless steels have the appropriate mechanical properties, such as a high ultimate tensile strength and a good corrosion resistance [3].

Duplex stainless steels (DSS) combine great mechanical performance and high corrosion resistance properties of austenitic and ferritic phases. They are widely used in various industrial sectors, such as oil and gas, desalination, pulp and paper industries [4]. DSS development has followed two different paths: the improvement of corrosion performance through the increase of chromium, molybdenum and nitrogen content (superduplex and hyperduplex grades) or the restraining of molybdenum (SAF 2304) and nickel content which lead to the growth of the so called “Lean” duplex family. In particular, the low nickel grades, including LDX 2101®, were developed with the aim of advantageously replacing austenitic stainless steels (AISI 304 and 316) in applications where high mechanical resistance and enhanced localized corrosion resistance are required [5, 6], but also, to some extent, to substitute carbon steels, where maintenance costs are significant [7].

LDX 2101® has a high mechanical strength, due to its microstructure and high nitrogen content, combined with resistance to pitting and crevice corrosion above austenitic grade 304L and very close to 316L [8]. Moreover, one of their main advantages with respect to medical applications is the decrease in the nickel hypersensitivity effect for patients undergoing orthodontic treatments [9]. These austenitic-ferritic wires can act as a substitute for the common commercial wires of austenitic stainless steels, with the advantage of reduced nickel content. Clinical experiences have shown that

corrosion of austenitic stainless steels orthodontic appliances in the oral cavity results in the release of metallic ions into the surrounding tissues. This may cause local irritations or systemic effects, which are among the principal causes of clinical failure. In particular, the adverse effect of nickel has been delineated, and is attributed to the allergic sensitization of many people to this element.

In recent years there has been an increase in the utilization of fluoridated toothpastes, prophylactic gels, and dental rinses to prevent plaque formation and caries development. The presence of fluoride ions in the mouthwash solutions brings with it aggressiveness in the attack on dental alloys. The commercially available fluoridated products contain high contents of fluoride ions (F^-), up to 0.1 *wt.*%, with pH values ranging between 7.2 and 3.2 [10, 11]. Additionally, many commercially available fluoridated gels contain even higher concentrations of fluoride ions, up to 1 *wt.*%, whereas pH ranges between 7.2 and 3.2 [12, 13]. The conscientious health-care provider needs to know the consequences of the effect of fluoride ions on dental metallic materials. Some authors [14 - 16] have found that fluoride ions affect the corrosion behavior of titanium and its alloys. According to Al-Mayouf et al. [17], the severity of the attack depends on both depends on both the concentration of fluoride ions and pH.

To our knowledge, no studies have yet been carried out to assess the influence of fluoride on the electrochemical corrosion of lean duplex stainless steels in terms of their suitability for orthodontic clinical applications. Earlier studies on NiTi-based orthodontic wires [18 – 21] have demonstrated the higher risk of corrosion in certain experimental conditions. The deterioration of the corrosion resistance of orthodontic wires has two consequence: the first is a loss of the physical properties which play in the success of the clinical treatment; the second is the release of Ni ions, which have been shown to be toxic and the causes of allergic reactions.

The aim of the present work is contributing to the understanding of the effect of fluoride on the electrochemical corrosion behavior of LDX 2101® duplex stainless steel. With this purpose, open circuit potential and electrochemical impedance spectroscopy measurements were carried out in

artificial saliva and with addition of NaF. The corrosion behaviour of AISI 316L stainless steel was also evaluated for comparison.

2. Experimental details

Electrochemical measurements were performed on a DSS LDX 2101® (supplied by Outokumpu) with the chemical composition (*wt.%*) reported in Table 1.

The test specimens were cut into discs of 15 mm diameter. The samples were ground with a sequence of 400 – 4000 grit emery paper and subsequently polished with alumina suspension to attain mirror-appearance, washed with Milli-Q deionized water (18.2 MΩ), ultrasonically cleaned and degreased in ethanol, and dried in air. Tests specimens were embedded in a Teflon PAR holder and employed as the working electrode (WE). The reference electrode (RE) was a saturated calomel electrode (SCE, 0.242 V *vs.* SHE) and the counter electrode (CE) was a large platinum sheet. All the potentials described in the text are relative to the SCE, unless stated differently. A three-electrode flat KO2354 PAR corrosion cell (volume 0.25 L) was used and the test specimen employed as a WE was exposed to the aggressive environment with an area of 1 cm^2. The electrochemical measurements were carried out in Fusayama artificial saliva (0.4 g NaCl, 0.4 g KCl, 0.795 g $CaCl_2$, 0.69 g NaH_2PO_4, 0.005 g Na_2S, 1 g urea, and distilled water up to 1000 ml) and with the addition of 1 *wt.%* NaF (corresponding to 4500 ppm F^-), which simulates the fluoride concentration typically found in fluoridated gels [12, 13]. The pH of both tested media was 5.0. The artificial saliva was naturally aerated and the experiments were conducted without stirring. The temperature was maintained at 37 ± 1 °C using a thermostatic bath.

Open circuit potential, E_{OC}, measurements were performed using a Solartron 1286 Electrochemical Interface controlled by a computer. The E_{OC} was continuously monitored during 168 h exposure. Electrochemical impedance spectroscopy (EIS) measurements were carried out at open circuit potential using an EG&G PAR system Model 2263 and the Power Suite program. The impedance spectra were acquired in the frequency range from 100 kHz to 10 mHz at seven points per decade.

The amplitude of the sinusoidal perturbation signal was 10 mV. EIS plots at the corrosion potential were collected for increasing exposure times to the aggressive environment. The impedance data were analyzed using the software for complex non-least squares (CLNS) fitting developed by Boukamp [22] and software *ZsimpWin 2.0* [23].

For comparison, electrochemical experiments were also performed on the AISI 316L stainless steel supplied by Johnson Matthey, London, UK. Its chemical composition (*wt.*%) is given in Table 2.

3. Results and discussion

The open circuit potentials, E_{OC}, variations with exposure time of AISI 316L and LDX 2101® in artificial saliva, and with the addition of 1 *wt.*% NaF, are shown in Figure 1.

The open-circuit potential of a metal varies as a function of time, but it stabilizes at a stationary value after a certain period of exposure. For this reason, our measurements of open-circuit potentials are performed during 168 h exposure to the aggressive environments. The nature of the metal-solution interface varies with time and, consequently, the open-circuit potential is no longer a characteristic of the metal. It also depends on the experimental conditions, particularly the electrolyte composition, the temperature and oxygen content of the electrolyte, and the surface state of the metal [24]. The alloys in the series with the most active (negative) potentials will generally tend to undergo more significant corrosion, while the other alloys (with positive values) will generally suffer less attack. The open-circuit potential is used as a criterion for the corrosion behavior [24]. Although this approach is qualitative and remains insufficient for a complete analysis, it allows an initial classification and indicates relative trends, specific to the experimental conditions of the test.

As shown in Figure 1, the open circuit transients measured for the two stainless steels have similar trends in both aggressive environments, where E_{OC} from the instant of exposure shifts with time in the positive direction, indicating a spontaneous passivation due to development of an oxide film [25]. This continues as a result of the predominance of the cathodic processes over the anodic ones until

the film acquires a stable thickness. The necessary electrons of the cathodic reaction are provided by the ionization of metal atoms (most probably Cr atoms) entering the oxide phase.

By comparing the profiles reported in Figure 1, it can be observed that the most positive E_{OC} values occur for the artificial saliva; this result is an indication that the spontaneous oxide film formed on both stainless steels in artificial saliva displays better corrosion protection characteristics than the oxide films formed in artificial saliva with the addition of fluoride. Moreover, the open-circuit potentials of LDX 2101® are less negative than those recorded on AISI 316L. This behavior indicates that the spontaneous oxide formed at the surface of DSS seems to offer better protection than the one formed on austenitic SS in both aggressive environments.

Corrosion damage results from electrochemical reactions, and electrochemical measurements can often reveal the corrosion mechanism. Electrochemical impedance spectroscopy (EIS) is a technique with a small perturbing signal, and which causes very little damage to the sample. EIS is essentially a steady-state technique that is capable of accessing relaxation phenomena where relaxation times vary over orders of magnitude, and permits single averaging within a single experiment to obtain high precision levels. Besides, the corrosion mechanism can be estimated by analyzing the measured electrochemical impedance spectrum [26, 27]. Impedance spectra were recorded with the AISI 316L electrode and the LDX 2101® electrode at the open circuit potentials. Since any interface undergoing an electrochemical reaction is typically analogous to an electrical circuit consisting of a specific combination of resistors and capacitors, the electrochemical systems under investigation can be described in terms of their electrical equivalent circuits (EECs). Thus, the first task was to identify the best-fit EEC, based on the used software, in order to establish the values for the circuit elements. The usual guidelines for the selection of the best-fit EEC were followed: (1) a minimum number of circuit elements were employed; (2) the χ^2 error was suitably low ($\chi^2 \leq 10^{-4}$), and the errors associated with each element were up to 5%.

Representative impedance spectra of AISI 316L and LDX 2101® in artificial saliva, and with the addition of 1 *wt*.% NaF, obtained at E_{OC} for different exposure times up to 168 h (1 week), presented as Nyquist plots, are reported in Figure 2. The general profile of the spectra is similar for both aggressive environments. The presence of fluoride only decreases the impedance without changing other aspects of the behavior, suggesting similar metal dissolution mechanism in the absence and presence of F^- ions. An analysis of the experimental data with standard simulation methods revealed that all impedance spectra show two overlapped time constants. The EEC selected to fit the experimental impedance data was the two-time-constant cascade, reported in Figure 3, which seems to be able to afford the most coherent physical interpretation of the results. It consists of the solution resistance of the aggressive environment, R_Ω, connected in series with two parallel resistor/constant phase element pairs, R_1/Q_1 and R/Q_2, where subscripts 1 and 2 designate the high and low frequency time constants, respectively. The value of R_Ω was found to be constant during the measurements, i.e. 280.0 Ω cm^2 in artificial saliva and 80.0 Ω cm^2 in artificial saliva + NaF. The parameter R_1 represents the resistance due to the ionic conduction through the passive film formed, coupled with a capacitance due to its dielectric properties, Q_1, R_2 corresponds to the charge-transfer resistance, R_{ct}, and Q_2 represents the double layer capacitance, C_{dl} [27, 28]. Constant phase elements (CPE, Q) were used in the EEC instead of capacitors to account for the effects of deviations to ideal electric behavior arising from electrode roughness and heterogeneities of the surface films [27].

The impedance of a CPE is defined as:

$$Z_{CPE} = \frac{1}{Y_0 (j\omega)^n} \quad (1)$$

where ω is the angular frequency and Y_0 is a constant, and the value of the exponent n, ranging $-1 \leq n \leq 1$, indicates the deviation from ideal capacitive behavior (e.g., when $n \approx 1$). Goodness of fitting was at high level. The standard deviation χ^2 was in the order of 10^{-4}, and the relative error of

each parameters was less than 5%. In Figure 2 measured impedance diagrams are denoted with scattered symbol and fitted diagrams with lines.

Figure 4 reports, for AISI 316L and LDX 2101®, the variation of polarization resistance, R_p, as a function of exposure time to the aggressive environment. The R_p value is calculated using [29]:

$$R_p = R_1 + R_2 \quad (2)$$

where R_1 and R_2 are parameters from the fitting procedure. The polarization resistance gives a suitable measure for the stability of the passive film. The R_p value increases during the first 72 h of exposure to the aggressive environment, after which it stays more-or-less constant. This confirms the stable passive layer on both the tested stainless steels, as evidenced for AISI 316L [28, 30]. As can be seen, the R_p is lower in the solution containing NaF for both the steels under investigation, having a slightly greater impact on the AISI 316L, than on the LDX 2101®. The value of the estimated R_p in artificial saliva after 72 h exposure is four times higher for AISI 316L, and three times higher for LDX 2101®, compared to the R_p values in artificial saliva with the addition of 1 *wt.*% NaF. This corresponds to the higher corrosion activity of the aggressive environment.

The variation of passive film capacitance, C_1, with time in both aggressive environments is shown in Figure 5. The C_1 values were calculated from Q_1 using the following equation [27]:

$$C_1 = (R_1^{1-n} Q_1)^{1/n} \quad (3)$$

As can be seen, the capacitance decreases slightly in the first 72 h, demonstrating that the passive film increases in the first 72 h and then tends to become stable. Estimates regarding the thickness of the formed film can be made by assuming a homogeneous composition of the oxide layer. Then, by considering the film to act as a parallel plate dielectric, the capacitance will be related to the thickness according to:

$$C_1 = \frac{\varepsilon_0 \, \varepsilon \, A}{d} \quad (4)$$

where ε_0 is the vacuum permittivity (8.85×10^{-14} F cm^{-1}), ε is the dielectric constant of the oxide, A is the effective area, and d is the thickness of the oxide layer [31]. Assuming $\varepsilon = 30$, which is the

value for thin films [30, 32], and the surface roughness factor as unity for an electropolished surface, the estimated values of d show that the layers formed on both stainless steels are typically a few nm thick, as can be seen in Figure 6. Though the obtained values can only be regarded as an estimation based on simple assumptions, they are in reasonable agreement with previous reports in the literature, which suggest that the passive films on stainless steels are very thin (1 – 3 nm) [32]. It can be observed that the thicknesses of the protective films on the LDX 2101® substrate are slightly higher than those on the AISI 316L. However, it is difficult to obtain accurate thickness values for the passive film using the capacitance; this is due to the dielectric constant, which is usually not well known and can vary when the composition of the film changes.

It is well known that the high corrosion resistance of stainless steels to various aggressive environments is ensured by the spontaneous formation of a protective surface oxide layer, which leads to a marked decrease in the dissolution kinetics of the underlying alloy [33 – 35]. This passive film is generally described as a mixed oxyhydroxide layer, composed mainly of Cr(III) species in the inner layer and Fe(III) species in the outer layer [32, 36, 37]. For a sufficient chromium content in the alloy [38, 39], preferential chromium oxidation and/or preferential iron dissolution leads to a significant Cr(III) enrichment in the oxide layer, conferring to the passive film its protective nature. The extent of chromium oxide enrichment during passivation strongly depends on the composition of the alloy [32, 39, 40]. It has been reported that the mole fraction of Cr-oxide increases with increasing chromium content in the alloy [34, 38, 39]. The role of the alloyed chromium in enhancing the passivity of the stainless steels is frequently explained in terms of a percolation model of passivation [41]. It is considered that the chromium forms insoluble Cr_2O_3, and a continuous network of Cr– O–Cr–O is then produced, which prevents the dissolution of iron. The addition of fluoride ions causes the surface films to become less stable and eventually a breakdown of the film may eventually occur. The fluoride ions are aggressive ions that degrade the protective oxide layer formed on

stainless steels. As a results of the complex formation of metal-fluoride molecules at the surface of the alloy, the oxide layer is consequently weakened [42].

As reported in Figure 4, the R_p values of the LDX 2101® are higher than the R_p values of the AISI 316L at E_{OC}; these results indicate that the spontaneous oxide film formed on the DSS exhibits higher stability than the oxide film formed on the austenitic SS in both aggressive environments. The corrosion rate is inversely related to R_p – the higher the value of R_p the higher the corrosion resistance (lesser corrosion rate). Therefore, the larger R_p values showed by the LDX 2101® respect to the AISI 316L highlight its higher stability in both aggressive environments, in agreement with the results obtained from open circuit potential measurements (Fig. 1). This could be ascribed to a strengthening of the passive oxide film due to the presence of higher amounts of chromium and nitrogen in the alloy, thus increasing its resistance to fluoride ions attack. On the other hand, the beneficial effects of nitrogen on passivity and corrosion resistance of stainless steels are well documented in previous studies. Nitrogen in an uncharged or negatively charged state was found to be enriched on the metal side of the metal/passive film interface as demonstrated by X-ray photoelectron spectroscopy (XPS) and Auger electron spectroscopy (AES) [43, 44]; this interface enrichment could act as a protective layer from the penetration of harmful ions, thereby increasing the passive film stability [45, 46].

Further studies about properties investigation and surface analyses of LDX 2101® are planned aiming to a deeper understanding of the protective behavior of its passive oxide film. Besides, Tsai et al. [47] have reported the galvanic corrosion of DSS in aggressive environments, i.e., in mixed H_2SO_4/HCl and HNO_3 solutions, due to the difference in the chemical composition between the ferritic and the austenitic phases. The galvanic corrosion of LDX 2101® was not considered in the present study; however, it is an interesting topic for future investigations, to assess the potential risk of galvanic corrosion between the ferrite and the austenite phases of LDX 2101® with respect to orthodontic applications.

4. Conclusions

The electrochemical corrosion behaviour of LDX 2101® duplex stainless steel together with the currently used AISI 316L metallic biomaterial was investigated for orthodontic clinical applications. Both steels were tested by 168 h open-circuit potential, E_{OC}, and electrochemical impedance spectroscopy (EIS) measurements performed in artificial saliva and with the addition of fluoride (1 *wt.*% NaF).

Open circuit potential, E_{OC}, values indicated that both DSS and austenitic SS undergo spontaneous passivation due to spontaneously formed oxide film passivating the metallic surface, in the aggressive environments. However, LDX 2101® presents higher E_{OC} values, indicating that its passive film seems to exhibit better corrosion protection characteristics than the one formed on AISI 316L.

The R_p values at E_{OC} strongly depend on the stability of the passive film, and it can be a measure of the corrosion resistance of the steel in the aggressive environment. In all cases the R_p values of the LDX 2101® are higher than those of the AISI 316L. R_p is found to increase for the first 72 h of exposure, after which it stays more-or-less constant. This confirms the stable passive layer on both stainless steels.

The thickness of the protective film is calculated form the capacitance parameter, C_1, and is found to be slightly higher on the LDX 2101® than on the AISI 316L.

The overall electrochemical data indicate a positive influence of alloy chemical composition on the corrosion behaviour of LDX 2101®. This could be ascribed to a strengthening of the passive oxide film due to the presence of higher chromium and nitrogen amounts in the alloy, thus increasing its dissolution resistance.

The experimental results show that the corrosion characteristics of LDX 2101® duplex stainless steel are better than those of AISI 316L austenitic stainless steel currently used as a biomaterial. This confirms the suitability of LDX 2101® for orthodontic applications in fluoride-containing artificial saliva, because its electrochemical stability is directly associated with biocompatibility.

5. References

[1] J.H. Potgieter, P.A. Olubambi, L. Cornish, C.N. Machio, E.S.M. Sherif, *Corros. Sci.* **2008**;50:2572

[2] M.A.M. Ibrahim, S.S.A. El Rehim, M.M. Hanza, *Mater. Chem. Phys.* **2009**;115:80

[3] T. Hryniewicz, R. Rokicki, K. Rokosz, *Corrosion* **2008**;64:660

[4] A. ItmanFilho, J.M.D.A. Rollo, R.V. Silva, G. Martinez, *Mater. Lett.* **2005**;59:1192

[5] B. Deng, Y. Jiang, X. Juliang, T. Sun, J. Gao, L. Zhang, W. Zhang, J. Li, *Corros. Sci.* **2010**;52:969

[6] R. Merello, F.J. Botana, J. Botella, M.V. Matres, M. Marcos, *Corros. Sci.* **2003**;45:909

[7] J. Charles, P.Chemelle, *Proc. of 8th Duplex Stainless Steels conference*, **2010**, Beaune, France, 13-15 October

[8] J. Olsson, M. Snis, *Desalination* **2007**;205:104

[9] N. Raison-Peyron, *Revue Francaise D. Allergol.* **2010**;50:S23

[10] A.M. Al-Mayouf, A.A. Al-Swayih, N.A. Al-Mobarak, *Mater. Corr.* **2004**;53:88

[11] A. Robin, J.P. Meirelis, *Mater. Corr.* **2007**;58:173

[12] F. Toumelin-Chemia, F. Rouelle, G. Burdairon, *J. Dent.* **1996**; 24:109

[13] N. Schiff, B. Grosgogeat, M. Lissac, F. Dalard, Biomaterials **2002**;22:1995

[14] M. Nakagawa, S. Matsuya, K. Udoh, *Dent. Mater. J.* **2001**;20:305

[15] Y. Fovet, J.Y. Gal, F. Toumelin-Chemla, *Talanta* **2001**;53:1053

[16] H.M. Shim, K.T. Oh, J.Y. Woo, C.J. Hwang, K.N. Kim, *J. Biomed. Mater. Res.* **2005**;B73:252

[17] A.M. Al-Mayouf, A.A. Al-Swayih, N.A. Al-Mobarak, A.S. Al-Jabab, *Mater. Chem. Phys.* **2004**;86:320

[18] K. Kaneko, K. Yokoyama, K. Moriyama, K. Asaoka, J. Sakai, M. Nagumo, *Biomaterials* **2003**;24:2113

[19] G. Rondelli, *Biomaterials* **1996**;17:2003

[20] I. Watanabe, E. Watanabe, *Am. J. Orthod. Dentofacial Orthop.* **2003**;123:653

[21] H.H. Huang, H.Y. Chiu, T.H. Lee, S.C. Wu, H.W. Yang, K.H. Su, C.C. Hsu, *Biomaterials* **2003**;24:3585

[22] B.A. Boukamp, *Solid State Ionics* **1986**;18/19:136

[23] B. Yeum, *Electrochemical Impedance Spectroscopy: Data Analysis Software*, Echem Software, **2001**, Ann Arbor

[24] C.W. Wagner, W. Traud, *Z. Electrochem.* **1938**;44:391

[25] A.M. Shams El-Din, N.J. Paul, *Thin Solid Films* **1990**;189:205

[26] G. Song, A. Atrens, X. Wu, B. Zhang, *Corros. Sci.* **1998**;40:1769

[27] E. Barsukov, J.R. Macdonald, *Impedance Spectroscopy*, 2nd Edition, **2005**, J Wiley & Sons, New York

[28] W. He, O.Q. Knudsen, S. Diplas, *Corros. Sci.* **2009**;51:2811

[29] J.R. Scully, *Corrosion* **2000**;56:199

[30] D. Wallinder, J. Pan, C. Leigraf, A. Delblanc-Bauer, *Corros. Sci.* **1999**;41:275

[31] J. Pan, D. Thierry, C. Leygraf, *J. Biomed. Mater. Res.* **1996**;30:393

[32] C.-O.A. Olsson, D. Landolt, *Electrochim. Acta* **2003**;48:1093

[33] I. Olefjord, L. Wegrelius, *Corros. Sci.* **1996**;38:1203

[34] P Keller, H.-H. Strehblow, *Corros. Sci.* **2004**;46:1939

[35] R.-H. Jung, H. Tsuchiya, S. Fujimoto, *Corros. Sci.* **2012**;58:62

[36] C.R. Clayton, Y.C. Lu, *J. Electrochem. Soc.* **1986**;133:2465

[37] J. Högström, W. Fredriksson, K. Edstrom, F. Björefors, L. Nyholm, C.-O.A. Olsson, *Appl. Surf.. Sci.* **2013**;284:700

[38] C. Calinski, H.-H. Strebhlow, *J. Electrochem. Soc.* **1989**;136:1328

[39] S. Haupt, H.-H. Strebhlow, *Corros. Sci.* **1995**;37:43

[40] I. Olefjord, L. Wegrelius, *Corros. Sci.* **1990**;31:89

[41] R.M. Souto, I.C. MirzaRosca, S. Gonzales, *Corrosion* **2001**;57:300

[42] Y. Oshida, C.B. Sellers, K. Mirza, F. Farzin-Nia, *Mater. Sci. Eng. C* **2005**;25:343

[43] Y.C. Lu, B. Randy, C.R. Clayton, R.C. Newman, *J. Electrochem. Soc.* **1983**;130:1774

[44] C.A.O. Olsson, *Corros. Sci.* **1995**;37:467

[45] R.C. Newman, Y.C. Lu, B. Randy, C.R. Clayton, *Proc. 9th Int. Conf. Metallic Corrosion*, Toronto, **1984**;3:394

[46] R.C. Newman, T. Shahrabi, *Corros. Sci.* **1987**;27:827

[47] W.-T. Tsai, J.-R. Chen, *Corros. Sci.***2007**;49:3659

Figure legends

Figure 1 – Corrosion potential vs. time profile for AISI 316L austenitic steel and LDX 2101® duplex steel after 168 h exposure to (a) artificial saliva and (b) artificial saliva with the addition of 1 *wt.*% NaF

Figure 2 – Representative Nyquist diagrams of AISI 316L austenitic steel and LDX 2101® duplex steel for various exposure times to (a) artificial saliva and (b) artificial saliva with the addition of 1 *wt.*% NaF

Figure 3 – Equivalent electrical circuit used for modelling the impedance spectra on the passive metal surface

Figure 4 – Polarization resistance, R_p, for AISI 316L austenitic steel and LDX 2101® duplex steel after different exposure times to (a) artificial saliva and (b) artificial saliva with the addition of 1 *wt.*% NaF

Figure 5 – Capacitance of the passive film, C_1, for AISI 316L austenitic steel and LDX 2101® duplex steel after different exposure times to (a) artificial saliva and (b) artificial saliva with the addition of 1 *wt.*% NaF

Figure 6 – Passive film thickness, *d*, estimates from EIS results measured for AISI 316L austenitic steel and LDX 2101® duplex steel after different exposure times to (a) artificial saliva and (b) artificial saliva with the addition of 1 *wt.*% NaF

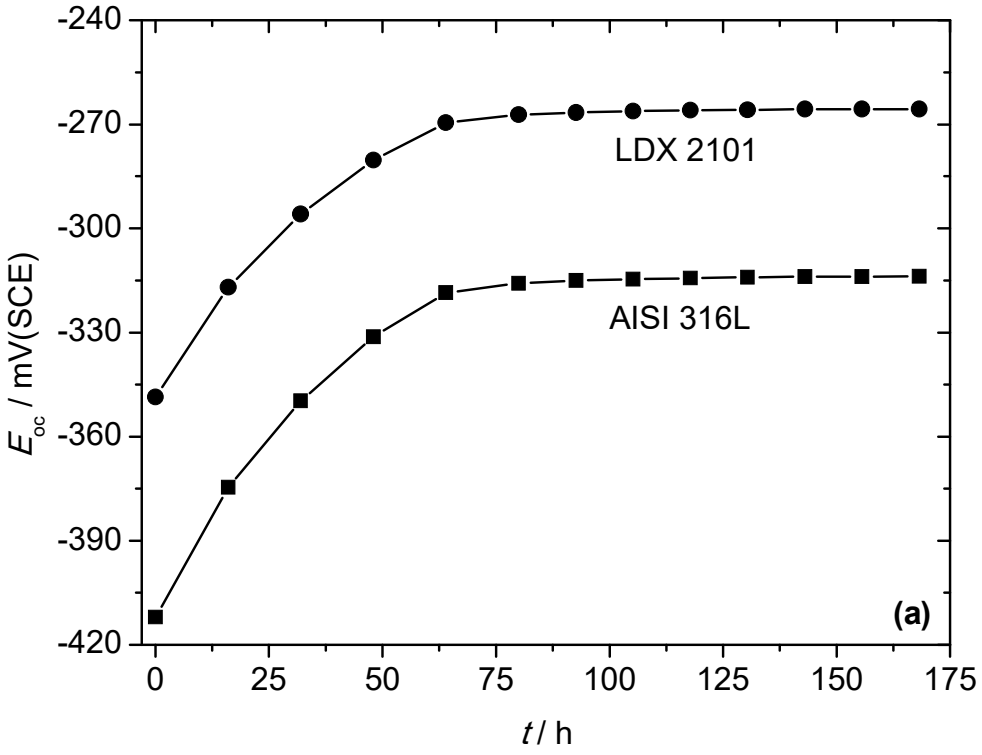
-240
-270
-300
-330
-360
-390
-420
E_{oc} / mV(SCE)
LDX 2101
AISI 316L
(a)
0
25
50
75
100
125
150
175
t / h

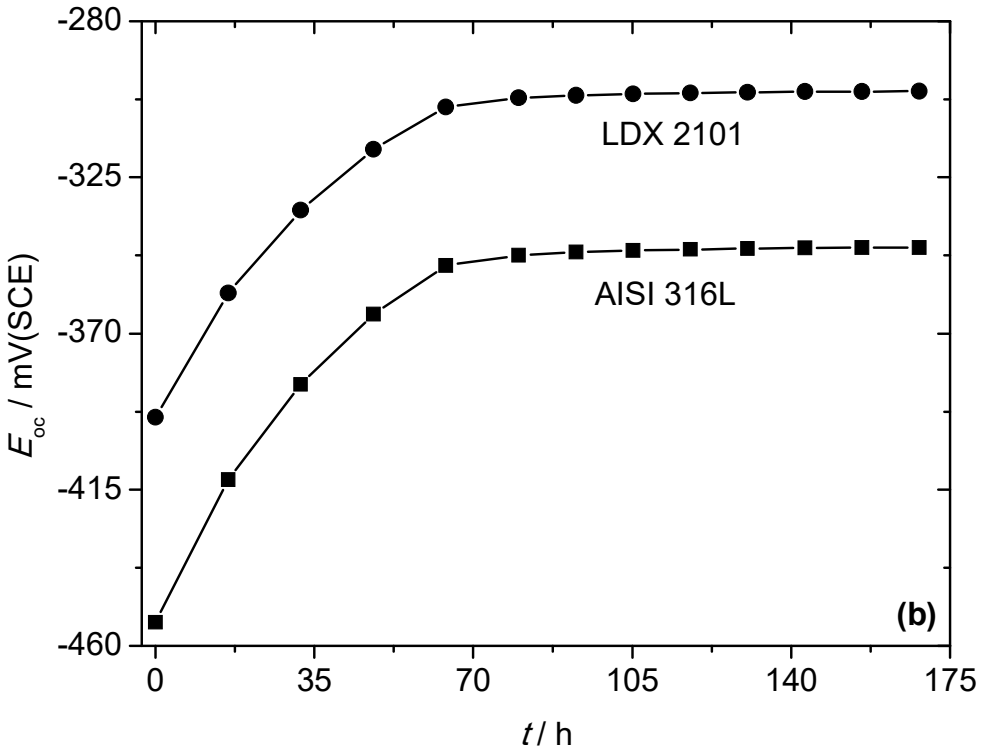
-280
-325
-370
-415
-460
E_{oc} / mV(SCE)
LDX 2101
AISI 316L
(b)
0
35
70
105
140
175
t / h

Figure 1

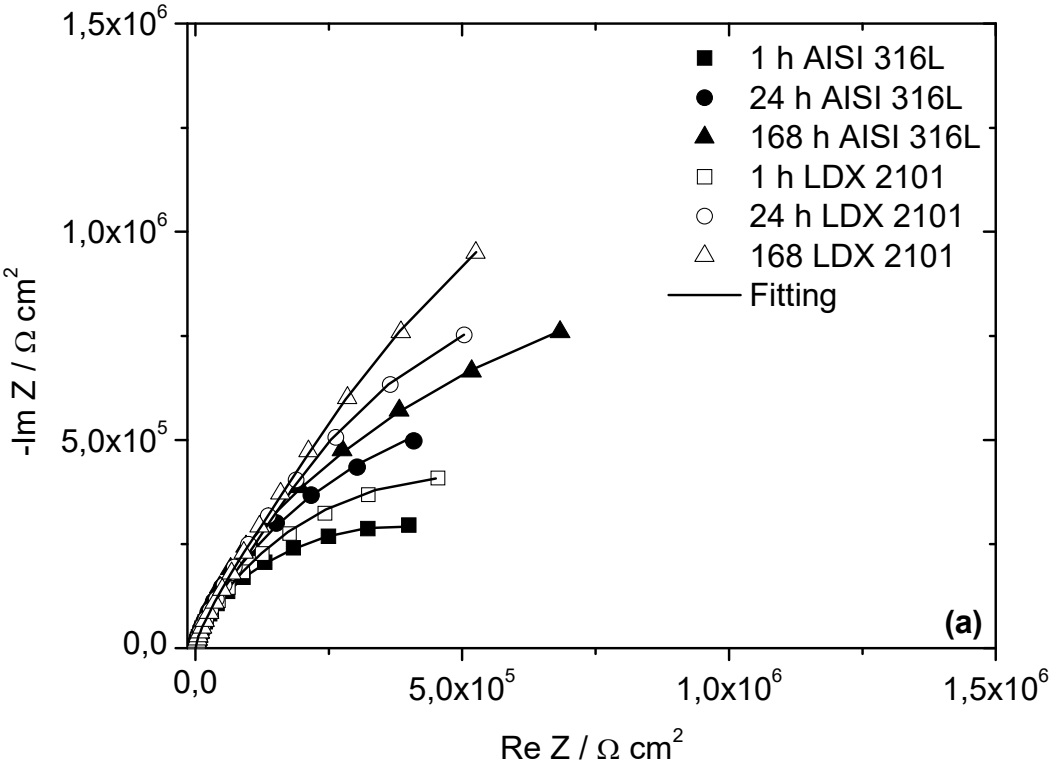
1,5x10^6
1,0x10^6
5,0x10^5
0,0
-Im Z / Ω cm^2
0,0
5,0x10^5
1,0x10^6
1,5x10^6
Re Z / Ω cm^2
1 h AISI 316L
24 h AISI 316L
168 h AISI 316L
1 h LDX 2101
24 h LDX 2101
168 LDX 2101
Fitting
(a)

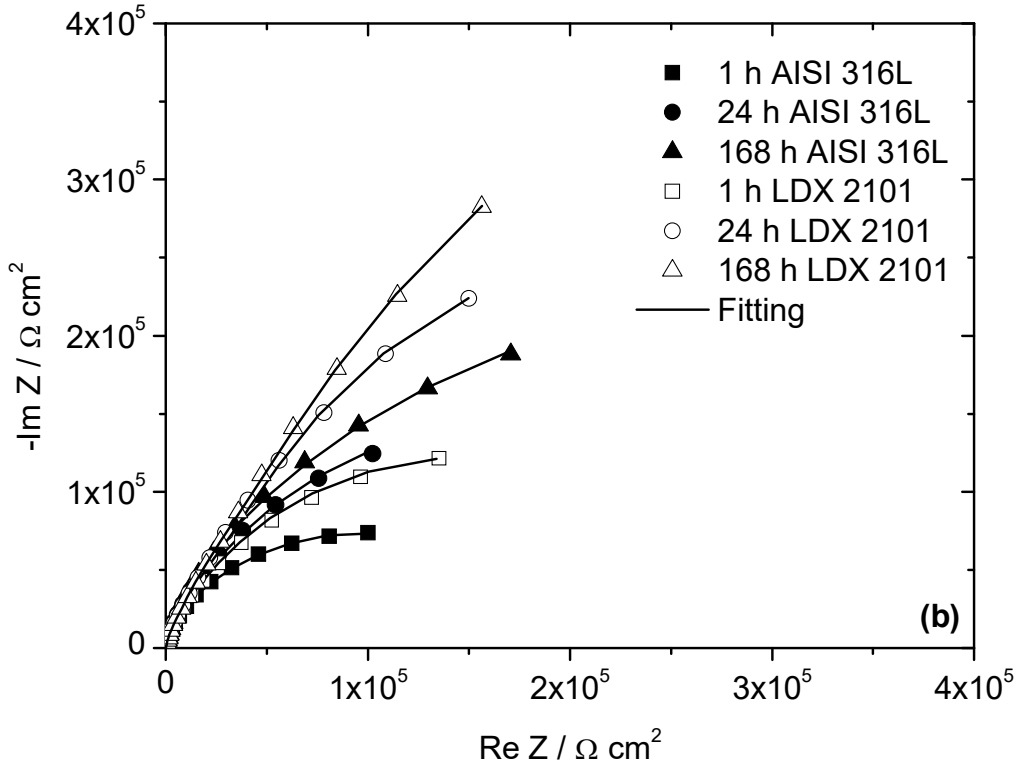
4x10^5
3x10^5
2x10^5
1x10^5
0
-Im Z / Ω cm^2
0
1x10^5
2x10^5
3x10^5
4x10^5
Re Z / Ω cm^2
1 h AISI 316L
24 h AISI 316L
168 h AISI 316L
1 h LDX 2101
24 h LDX 2101
168 h LDX 2101
Fitting
(b)

Figure 2

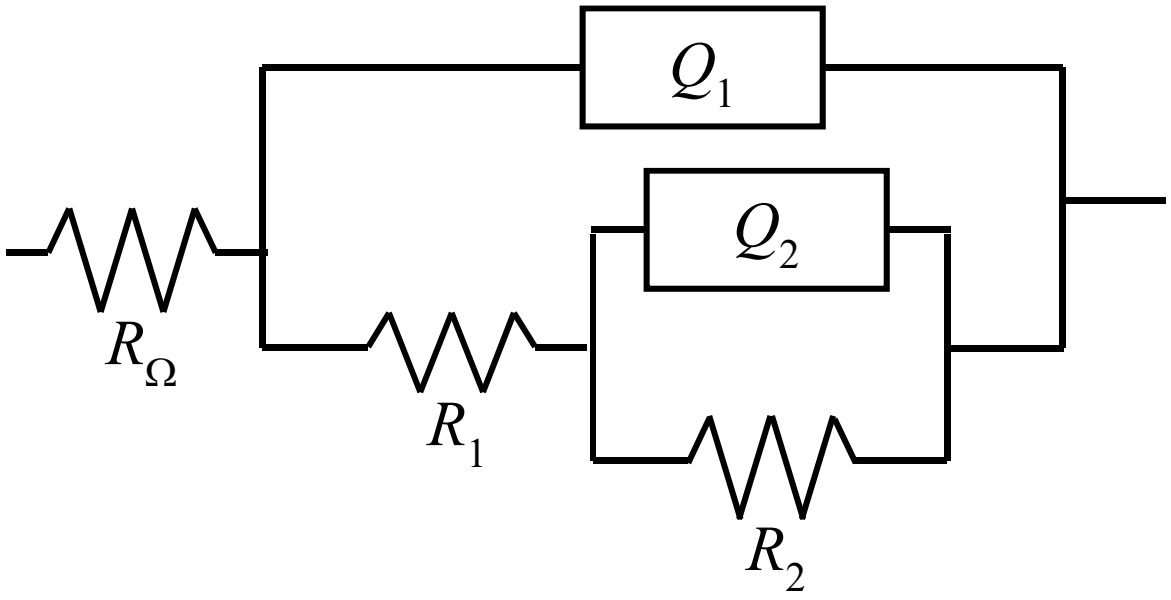

Figure 3

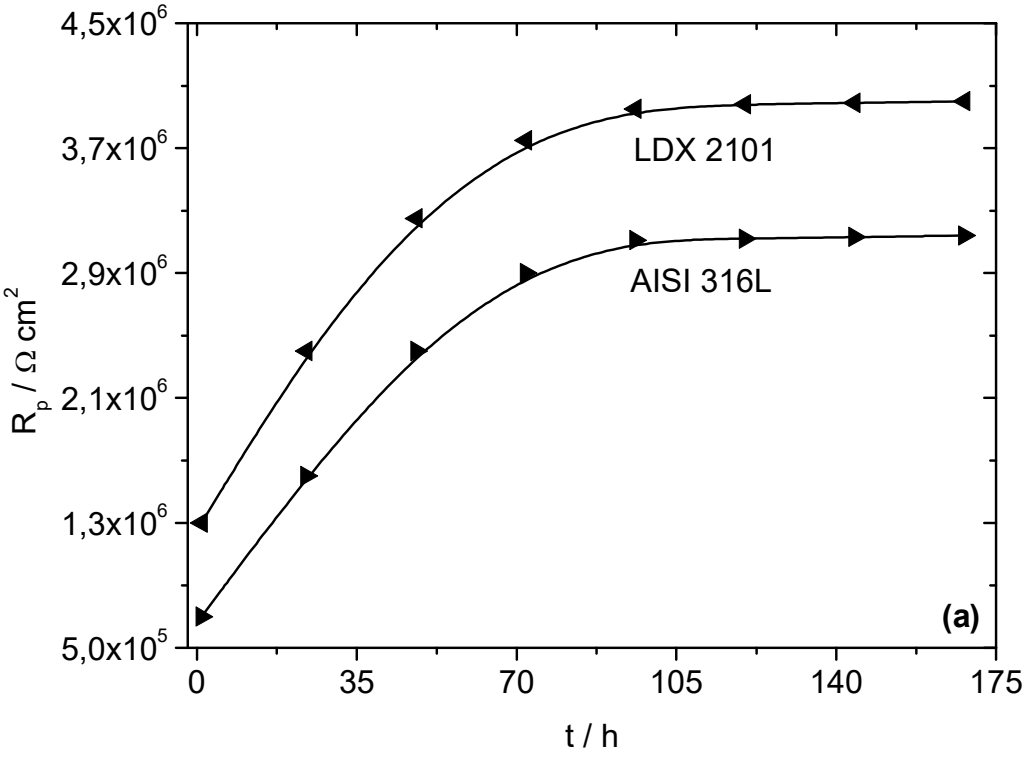
4,5x10^6
3,7x10^6
2,9x10^6
2,1x10^6
1,3x10^6
5,0x10^5
R_p / Ω cm^2
LDX 2101
AISI 316L
(a)
0
35
70
105
140
175
t / h

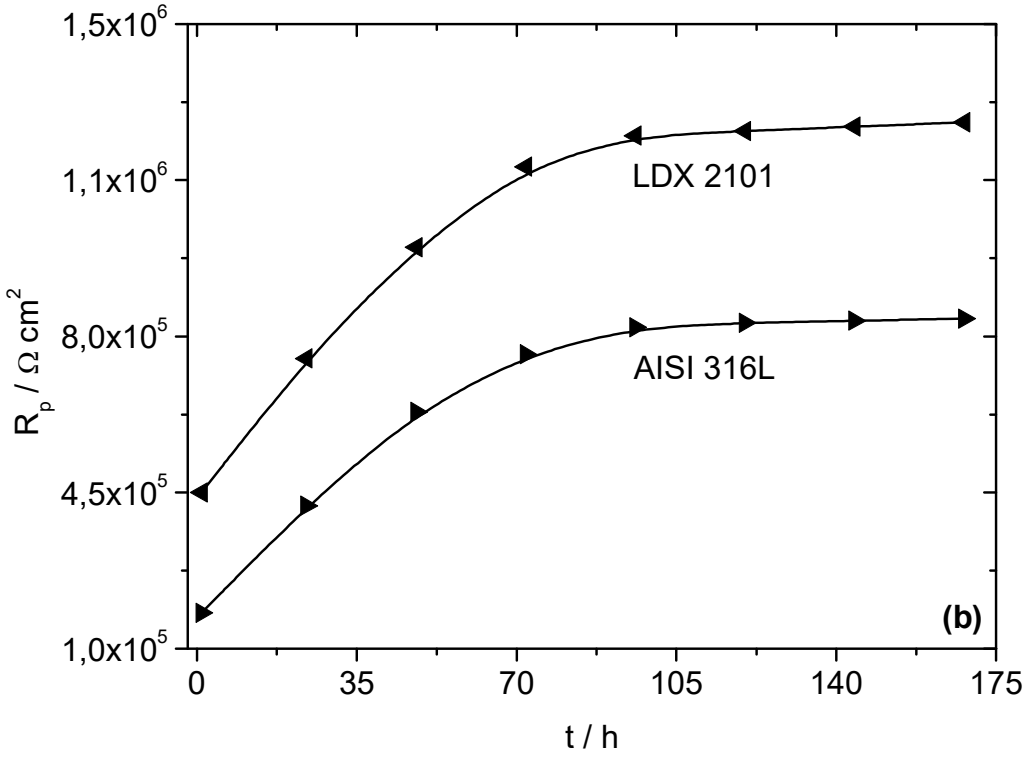
1,5x10^6
1,1x10^6
8,0x10^5
4,5x10^5
1,0x10^5
R_p / Ω cm^2
LDX 2101
AISI 316L
(b)
0
35
70
105
140
175
t / h

Figure 4

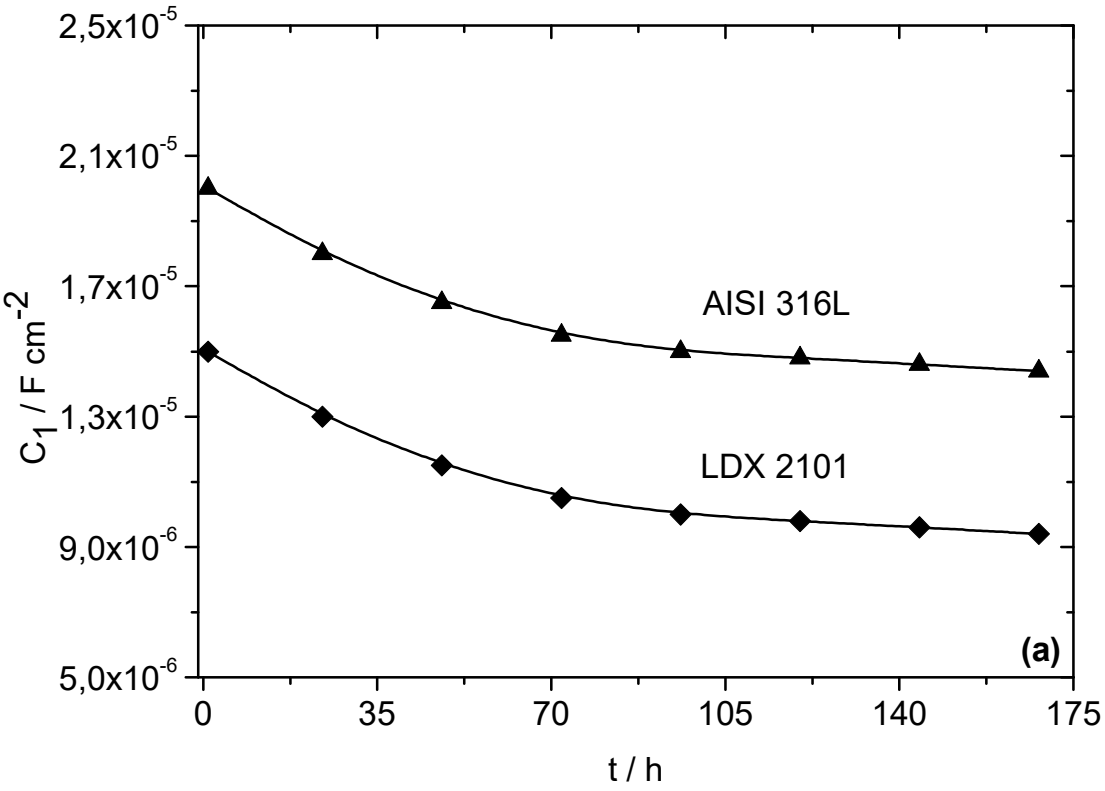
2,5x10-5
2,1x10-5
1,7x10-5
1,3x10-5
9,0x10-6
5,0x10-6
C1 / F cm-2
AISI 316L
LDX 2101
(a)
0
35
70
105
140
175
t / h

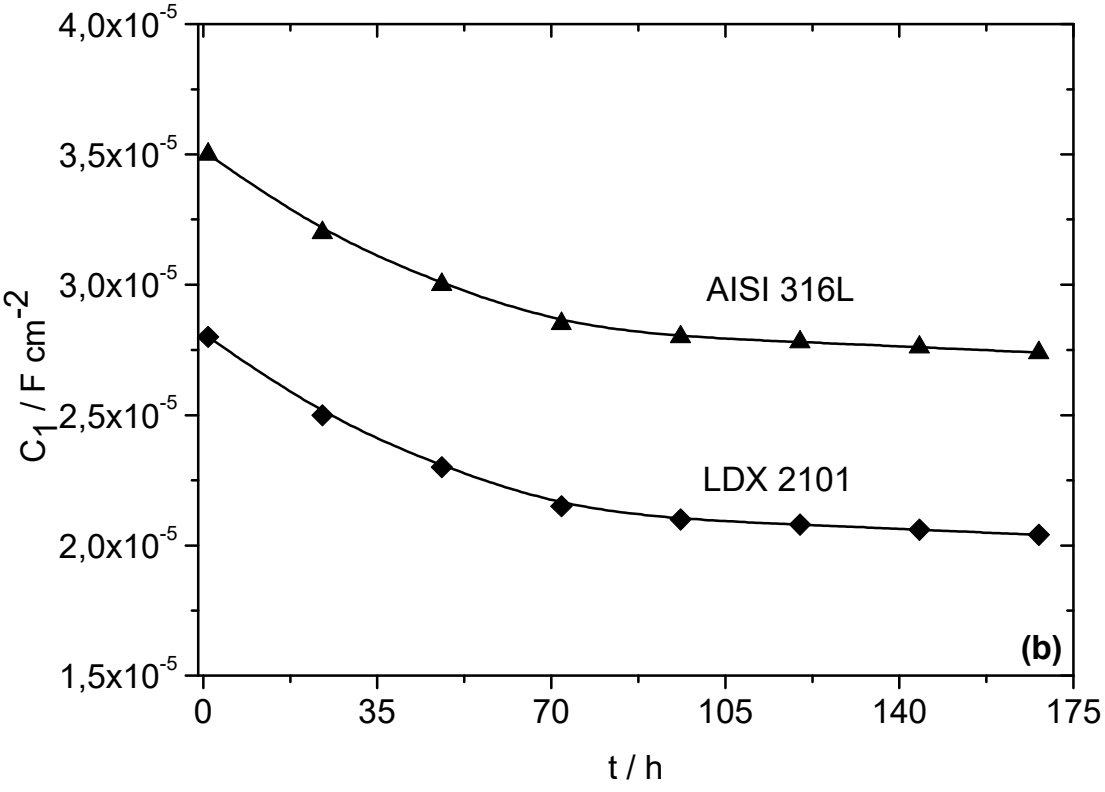
4,0x10-5
3,5x10-5
3,0x10-5
2,5x10-5
2,0x10-5
1,5x10-5
C1 / F cm-2
AISI 316L
LDX 2101
(b)
0
35
70
105
140
175
t / h

Figure 5

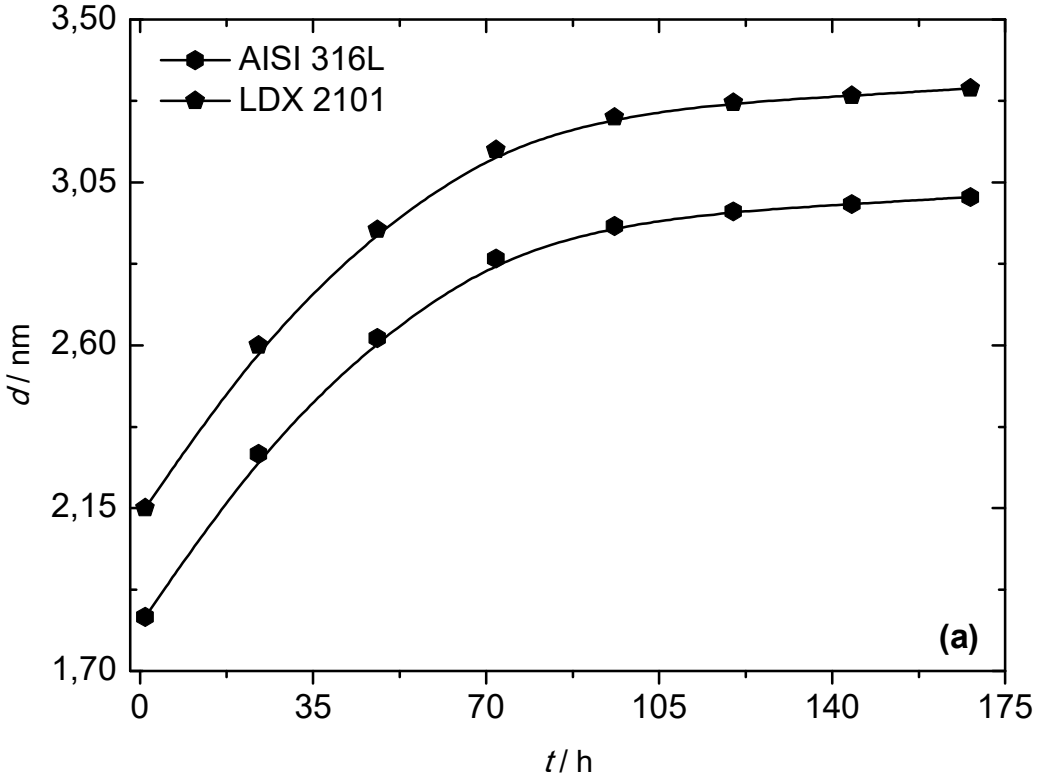
3,50
3,05
2,60
2,15
1,70
d / nm
AISI 316L
LDX 2101
(a)
0
35
70
105
140
175
t / h

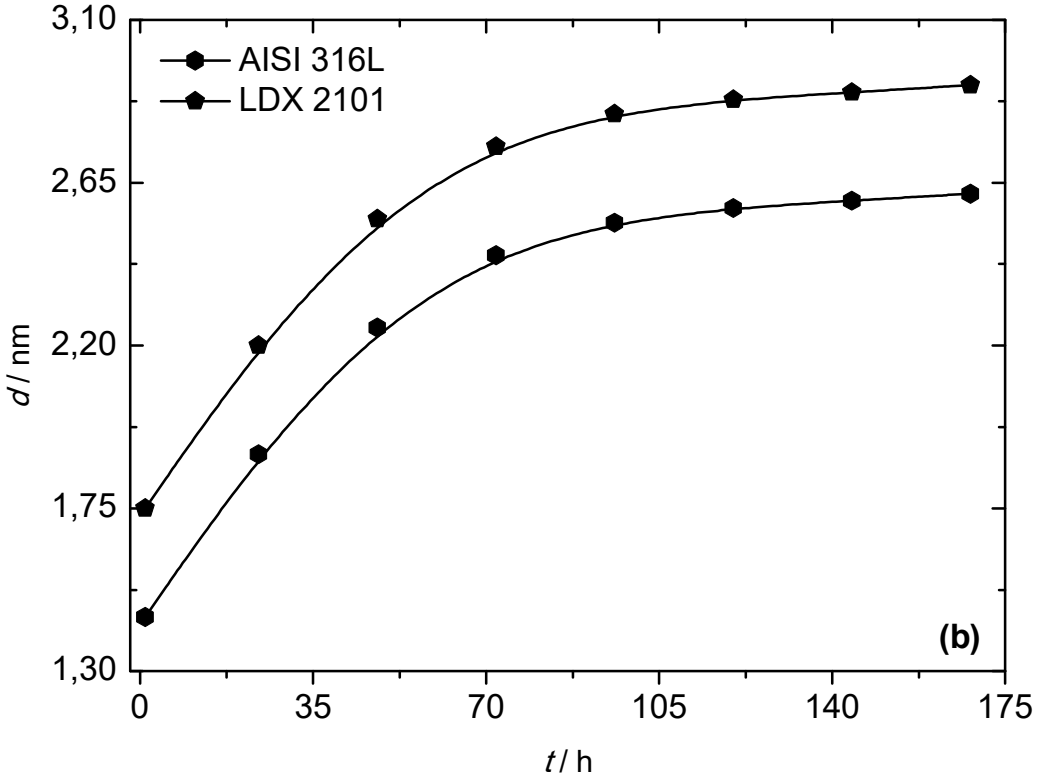
3,10
2,65
2,20
1,75
1,30
d / nm
AISI 316L
LDX 2101
(b)
0
35
70
105
140
175
t / h

Figure 6

Table 1 – Chemical composition (*wt.%*) of LDX 2101® duplex stainless steel

Elements	**Cr**	**Ni**	**Mn**	**Si**	**C**	**Mo**	**N**
%	21.47	1.19	5.72	0.29	0.027	0.35	0.23

Table 2 – Chemical composition (*wt.%*) of AISI 316L austenitic stainless steel

Elements	**Cr**	**Ni**	**Mn**	**Si**	**C**	**Mo**	**N**
%	17.01	10.06	1.40	0.38	0.020	2.10	0.04